One Inch Thermal Bubble Jet Printhead With Laser Structured Integrated Polyimide Nozzle Plate

Timo Lindemann, Heidi Ashauer, Ying Yu, *Member, IEEE*, Duccio Spartaco Sassano, Roland Zengerle, and Peter Koltay

***Abstract*—This paper reports on a novel 1/3 and 1-in thermal bubble jet printhead with integrated nozzle plate. The printheads are made by a combination of a standard printhead substrate with a new three-dimensional (3-D) structured polyimide nozzle plate avoiding a three-layer assembly known from other commercial printheads. The 50-μm- (respectively, 75-μm)-thick nozzle plate contains the fluidic channels and 208 (respectively, 312) nozzles with minimum lateral dimensions of 10 μm. The misalignment of the two laser structured layers has proved to be less than 1μm. The nozzle plate is assembled with the substrate using a 3-μm-high adhesive layer with an alignment accuracy of 5 μm. The integrated nozzle plate leads to a better control of the printhead geometry and saves one processing step in production. A 1/3-in as well as a 1-in design were studied because it was not sure if the 1-in design survives the fabrication of the silicon substrate. The powder blasting of the ink feeding slot was considered as critical process step. To predict the effect of misalignments or variations in the adhesive layer during the assembling process on the characteristic inkjet parameters—like droplet volume, droplet velocity, droplet quality, or print frequency—computational fluid dynamic (CFD) simulations have been performed. For these purposes, a fully three-dimensional model was set up using the volume of fluid method. The presented CFD model in combination with the applied pressure boundary condition substituting the behavior of the exploding vapor bubble provides a valuable possibility to simulate media variations, actuation variations, as well as 3-D related geometrical variations. The differences in ejected droplet volume and droplet velocity between simulation and experiment are below 5%. Conclusively, the innovations presented in this paper are as follows. The presented printhead layout designed by Olivetti I-Jet provides an improved print frequency compared to commercially available printhead designs. The 1-in integrated nozzle plate and the required innovative fabrication technology offers a tripling of the printing speed compared to a conventional 1/3-in design only by means of an increased printing area. The new fabrication and packaging approach offers the reduction of processing and assembling steps leading to a better control of the printhead geometry. The CFD simulations provide a three-dimensional approach to estimate the influences of manufacturing and adjustment tolerances. [1723]**

Manuscript received November 22, 2005; revised October 2, 2006. This work was supported by the Federal Ministry of Education and Research (BMBF), Germany, under Grant 16SV1607 within the EURIMUS program (IDEAL EM 42). Subject Editor C.-J. Kim.

T. Lindemann and P. Koltay are with the Laboratory for MEMS Applications, Department of Microsystems Engineering (IMTEK), University of Freiburg, D-79110 Freiburg, Germany (e-mail: lindeman@imtek.de; koltay@imtek.de).

H. Ashauer is with HSG-IMIT, D-78052 Villingen-Schwenningen, Germany.

Y. Yu is with Boehringer Ingelheim microParts, D-44227 Dortmund, Germany.

D. S. Sassano is with Olivetti I-Jet, 11020 Arnad, Italy.

R. Zengerle is with the Laboratory for MEMS Applications, Department of Microsystems Engineering (IMTEK), University of Freiburg, D-79110 Freiburg, Germany. He is also with HSG-IMIT, D-78052 Villingen-Schwenningen, Germany.

Digital Object Identifier 10.1109/JMEMS.2007.892796

***Index Terms*—Bubble jet printhead, computational fluid dynamic (CFD) simulation, inkjet, integrated nozzle plate, laser machining, volume of fluid (VOF).**

I. Introduction

HIGH-quality color image, low machine cost, and low printing noise are the main advantages of inkjet printers. This has led to a rapid expansion of this technology in recent years. The two competing actuation principles of these so-called drop-on-demand printers are the piezoelectric driven printhead as reported in [1] and the thermally actuated bubble jet printhead developed in the 1980s [2]. Currently the bubble jet printer stands out with low manufacturing costs at comparable print quality. The aim of manufacturers and many researchers is the further optimization concerning maximum print frequency, active area of the printhead, resolution, and quality of ejected droplets [3]–[9]. This requires a further miniaturization and improvement of the printhead geometry including fluid channels, heaters, and nozzles to achieve an ideal printhead performance. Furthermore, the number of nozzles and the printhead size should be increased to gain printing speed. An important tool for the optimization is the simulation of the complete device, which is very cost- and time-effective compared to experimental hardware optimization. With computational fluid dynamics (CFD) simulations, a variety of relevant parameters like geometrical dimensions and ink properties can be investigated. Also the use of integrated nozzle plates is beneficial for the efficiency improvement of the printhead, as will be shown in the following.

II. Integrated Nozzle Plate

The integrated nozzle plate with two precisely aligned structural layers is made by an advanced laser ablation process considering an adequate design of the fluidic supply, which is of outstanding importance to achieve high print frequencies [10]. This design was designed by Olivetti I-Jet using a network simulation approach regarding a maximum print frequency. Due to this, the print frequency could be increased from 12 to over 15 kHz. The critical part of this print frequency optimization is that the fluidic resistance and the fluidic inertance of the supply channels have to be designed properly. However, they cannot be handled independently because both are depending on the length of the supply channels. For a fast refilling of the nozzle chamber after ejection, a small fluidic resistance would be preferred, whereas for the ejection, a high fluidic resistance would be preferred to inhibit the flow in backward direction. This tradeoff could be

handled by the fluidic inertance, which acts as an additional fluidic resistance at high frequencies.

The integrated nozzle plate avoids a generally used three-layer design where the first layer includes the electronics and the heaters, the second layer contains the fluidic parts like channels or nozzle chambers, and the third layer has the nozzle plate with usually laser drilled nozzles [11]. However, additional advantages of the two-layer design are the reduction of processing steps and the necessity of only one assembling step. Due to this, smaller fluidic structures can be realized, leading to a better control of the printhead geometry and to improved optimization opportunities for the ejection process. Furthermore, the fabrication of such printheads could be cheaper and more reliable compared to conventional printheads. Moreover, with the presented design, the print frequency could be increased from 12 to over 15 kHz and the droplet velocity could be increased from 10 to 12 m/s compared to commercially available printheads from Olivetti I-Jet.

One possible approach to meet the demands of high printing speed is to use a much wider printhead in order to address a larger area in the same time. A 1-in printhead with integrated nozzle plate provides a realistic and cost-effective solution to this problem. The 1-in printhead triples the printing speed compared to a 1/3-in design only by means of increasing the printed area during one cycle of the print cartridge. To achieve such a large printhead with integrated nozzle plate is, however, very challenging because of the high requirements concerning the fabrication technology of the nozzle plate, the alignment of nozzle plate and substrate, and the assembly of the printhead. The results reported in the following provide suitable solutions to all of these problems.

A. Laser Machining

An excimer laser with a wavelength of 248 nm was used to structure different designs of integrated nozzle plates. A 1/3-in nozzle plate and finally a 1-in nozzle plate with different channel/nozzle dimensions and different foil thickness were fabricated, respectively.

The 1/3-in nozzle plate has been processed by using a commercial excimer laser system (LPX 305 made by Lambda Physik AG).[1] But the structured area of a 1-in nozzle plate exceeds the exposure area of typical commercial systems for excimer laser ablation. The whole structured area of a 1-in nozzle plate must be first divided into several parts; then the laser has to step these parts sequentially. This can easily be realized for the nozzle layer. The channel layer however, is a whole area without any break. A stepping process would produce overlaps between the subareas. To avoid this, a full-scale scanning process was developed for lasering the channel layer. Also the used laser system was modified to get improved behaviors in order to realize the new process. With this process, the nozzle plate was structured by two-dimensional scanning "on the fly." The fabrication time of a 1/3-in nozzle plate takes about 20 s, whereas the fabrication time of the 1-in nozzle plate takes about 90 to 100 s due to the threefold stepping during the laser ablation process.

[1]http://www.lambdaphysik.com

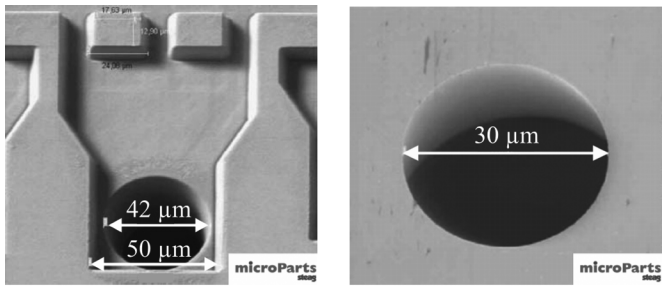

Fig. 1. Full-scale lasered 1/3-in nozzle plate consisting of two precise aligned structural layers. The nozzle chamber, ink channel, and the nozzle. View from the (a) inlet and (b) outlet, respectively.

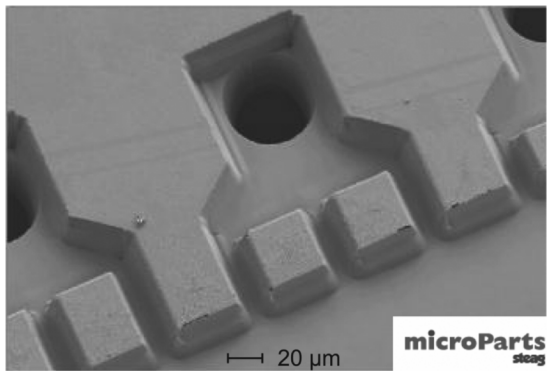

Fig. 2. View from the inlet of a full-scale lasered 1-in nozzle plate consisting of the two precise aligned structural layers.

The 50- and 75-μm-thick polyimide foils (for the 1/3- and 1-in nozzle plater, respectively) were structured successfully in two precisely aligned structural layers by the two-dimensional scanning process in combination with the sequential nozzle stepping. The two masks required contain the nozzle chamber with the ink channels and the nozzle, respectively. The misalignment of the two laser processes is less than 1 μm. A scanning electron microscope (SEM) picture of one nozzle chamber of the 1/3-in nozzle plate is depicted in Fig. 1(a), and the corresponding nozzle outlet is displayed in Fig. 1(b). An excellent sharpness of the edges and planar surfaces can be observed. In Fig. 2, a similar picture for the 1 in nozzle plate is displayed.

To fulfill the specifications of different nozzle and chamber designs, the draft angle of the lasered structures can be varied between 7° and 28° by varying the energy density of the laser pulse in a certain range and, in addition, by using other techniques such as a wobble plate in the laser optics. The draft angle also depends on the material of the nozzle plate and the ablation depth. In Fig. 3, a vertical cut through the 1/3-in nozzle plate is displayed. The void was filled with a filler material to avoid damage of the structure during preparation. The nozzle exhibits a typical draft angle of about 8°, and the chamber shows clearly the two structural layers with different heights.

B. Surface Treatment

After the laser machining of the nozzle plates, various treatments of the surfaces are required. On the one hand, a

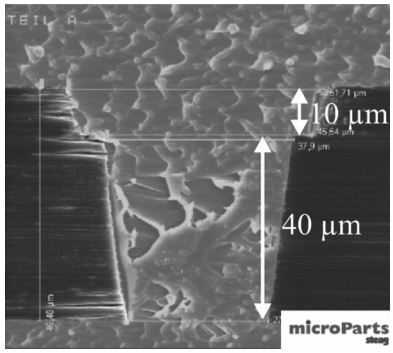

Fig. 3. Vertical cut through the two structural layers of the 1/3-in nozzle plate with a nozzle chamber and nozzle filled with a filler material (light area) to avoid the damage of the structure.

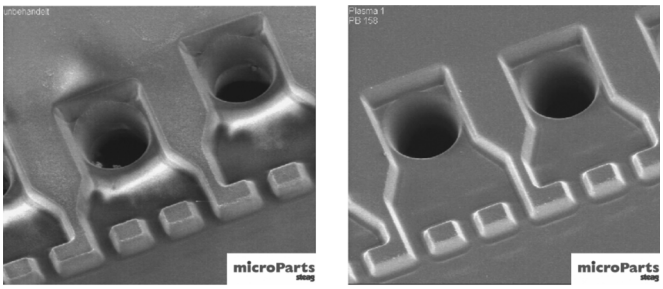

a) b)

Fig. 4. Laser structured 1/3-in nozzle plate (a) before and (b) after the cleaning in an oxygen plasma.

cleaning of the laser entry side is necessary to remove the remains of the laser process. Therefore, different kinds of cleaning processes—such as cleaning with organic/inorganic solvent, ultrasonic cleaning, and plasma cleaning using oxygen (O_2), oxygen-argon $(O_2 - Ar)$, or oxygen-tetrafluoromethane $(O_2 - CF_4)$, and combinations of those processes—were tested to prove the best purification. It is well known that in a plasma cleaning process, the parameter set (pressure, temperature, gas flow rate, process duration field density, and frequency) plays an important role. Process optimization for the nozzle plate cleaning has been made successfully with a commercial system. The best result was obtained using the oxygen plasma in combination with a suitable precleaning as depicted in Fig. 4 before and after the cleaning.

On the other hand, a surface treatment of the front side of the nozzle plate is necessary to provide an adequate hydrophobicity. The contact angle of the front side could be increased to up to 95° applying a wet chemical treatment using a commercially available chemical solution. This leads to a chemical modification of the surface with increased hydrophobicity. A better long-term stability compared to conventional plasma treatments could be proven by long-term storage tests and ink saturated storage tests. After storing of three months, no reduction of the contact angle could be observed. Ink-saturated storing also leads to no significant reduction of the contact angle.

III. Assembling

The major challenges for completing the printhead are the assembly of the structured nozzle plate with the silicon chip and

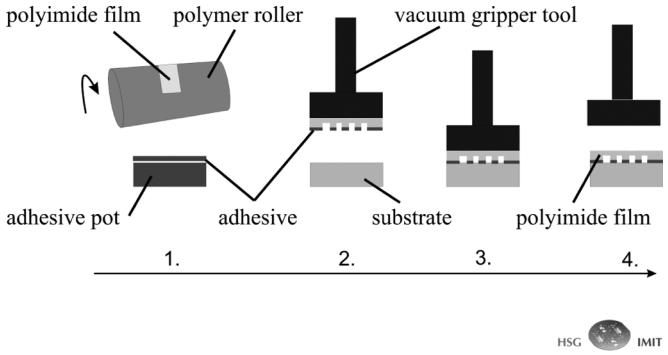

Fig. 5. Schematic illustration of the adhesive roller transfer process. 1. Picking up adhesive out of a pot directly on the polyimide film using a polymer roller. 2. Picking the coated polyimide film using a vacuum gripper tool. 3. Alignment on the substrate. 4. Finally removing the gripper tool.

the requirement of a minimum height of the adhesive to guarantee the maximum printhead performance. Especially when depositing adhesive layers with a thickness of less than 10 μm, one has to face two major challenges. First is the depositing process itself. Secondly, the properties of the resulting thin layer of adhesive can significantly differ from the characteristics of the bulk material. Reasons for this behavior can be found in the domination of surface effects towards structural properties of the bulk material, inhibition of oxygen from the surrounding atmosphere, and possible evaporation of solvents or hardeners.

Different approaches were analyzed to coat the substrate provided by Olivetti I-Jet[2] with a homogenous thin adhesive layer. Applying different well-known procedures of coating like spraying, spinning, capillary transport, and transfer techniques, different types of epoxy-based adhesives were studied. Epoxy was chosen because of the suitable media properties and good adhesion abilities. The main challenges are the prevention of bubble embedding, lacking bond strength, and plugging of the fluid channels.

Finally, the best performance was achieved using a roller transfer technique as illustrated in Fig. 5. To achieve a homogeneous adhesive transfer, the polyimide needs to be cleaned properly. This was achieved by low-power ultrasonic cleaning first in acetone and then in isopropanol. A subsequent exposure to an oxygen plasma created free bonds at the surface of the polyimide film, increasing the surface activity and thus its affinity to the adhesive. The adhesive was filled into a 5-μm-deep reactive ion etched silicon pot and leveled out by a doctor blade. Using a metal roller, the structured polyimide nozzle plate was subsequently coated with adhesive. Once leveled, the adhesive can be used for 15 min due to an increase in adhesive viscosity. The reason for this rapid increase in viscosity in thin layers relates to the evaporation of unreacted hardener. A flip-chip bonder from FineTech GmbH[3] was used to transfer the coated polyimide film onto the printhead substrate with an alignment accuracy of 5 μm without clogging of the fine structures (see Fig. 6). The adhesive Epotek 353ND by Polytec[4] showed adequate performance to create a layer

[2]http://www.olivettii-jet.it

[3]http://www.finetech.de

[4]http://www.polytec.com

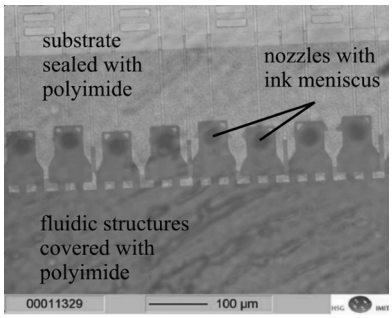

Fig. 6. Assembled nozzle plate on printhead substrate. The dark areas are ink-filled fluidic structures, whereas the light areas represent leakproof joined areas. The ink meniscus inside the nozzles can be seen as dark discs.

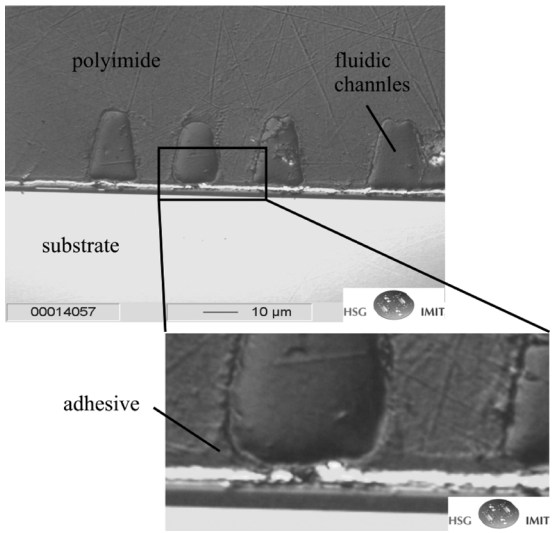

Fig. 7. Cut through an assembled printhead showing the polyimide film sealed on the substrate without clogging the fluidic channels.

thickness of approximately 3 μm. After an adequate curing process of 90 min at a temperature of 85 °C, satisfactory bond forces were obtained.

In this stage of the project, the printhead prototypes exclusively were fabricated manually. According to this, the fabrication yield was not optimized at this stage and not determined quantitatively. The laser ablation, however, exhibits a 100% yield. The assembling yield could definitely be improved by an automated fabrication chain. Such an automated mass production of the printheads is feasible using the applied fabrication steps but was not approached yet.

To prove the successful assembling of the integrated nozzle plate, different tests have been performed. First, the capillary filling of the printhead was studied using an optical observation as displayed in Fig. 6.

Furthermore, a cut through the channel structures inside the nozzle plate, as shown in Fig. 7, was analyzed. The trapezoid cross-section of the channels, the adhesive layer, and also a slight capillary wicking by adhesive can be seen. The adhesive that got into the chamber and rounded the chamber inner corners potentially could influence the first capillary filling of the printhead. The rounding could slow down the capillary filling because the capillary pressure could slightly decrease due to the change of the cross-section shape. The effect of such a rounding of the corners was not analyzed by means of simulations. However, no problems were observed during the experimental testings of the prototypes in respect thereof. Furthermore, the potential rounding of the supply channels does not affect the operation of the printhead because the ink meniscus does not get back in the supply channels. Only in this case a different capillary pressure would influence the printhead performance. The increase of the fluidic resistance due to the decrease of the channel cross-section, which is the important parameter during operation, is very small and thus can be neglected.

Finally the functionality of the printhead was analyzed by operating single nozzles at different frequencies and taking stroboscopic pictures, which are illustrated in Fig. 8(a) and (b) for the 1/3- and 1-in printhead, respectively. After operation and cleaning with acetone in an ultrasonic basin, the printhead demonstrates a good and reproducible functionality that indicates the robustness of the assembling process. Also after standardized temperature (DIN IEC 68 214), humidity (DIN IEC 68 256), and ink-saturated storing, the devices worked properly with a deviation of the droplet volume of less than 5% before and after the storing for the same nozzles within the 1/3-in devices. No long-term operation tests were performed. However, some of the prototypes were intensively characterized at high print frequencies. Due to this, at least 2 000 000 droplets were ejected without any symptoms of aging or failure.

In order to estimate the effect of the inevitable adjustment tolerances on the printhead performance, simulations of the droplet ejection have been performed, which are presented in the next section. Also. the effect of variations of ink parameters like density, viscosity and surface tension was analyzed.

IV. Simulation

Due to the complexity of the ejection process of a thermally actuated bubble jet printer, including heating of the microheater, bubble nucleation, collapse of the vapor bubble, and the actual droplet ejection [12]–[19], no complete physical simulation could be accomplished so far. The simulation task is typically modelled separately for actuation and ejection. To model the actuation, an appropriate pressure boundary condition proposed by Asai *et al.* [20]–[24] was applied. Using this pressure pulse as input for the simulation package ACE+ of ESI-Group [25], a CFD simulation has been set up and the droplet ejection process has been studied [25]–[28]. To examine the influences occurring in the real device, a complete three-dimensional model, instead of a simplified two-dimensional nozzle, was used. For instance, this can be the effects of asymmetric ink inlet channels or a nonspherical bubble shape. But also the effects appearing at problematic parts of the printhead geometry—for example, problems of the capillary refilling at convex edges or transitions between the angular nozzle chamber and the round nozzle—can be examined in three-dimensional (3-D) simulations. A further advantage of the three-dimensional model is that the realistic flight path of the droplet can be studied in dependence on the whole geometry. Furthermore, a possibly occurring divergence of the trajectory due to a misalignment or other geometrical reasons could also be studied using the presented 3-D simulation procedure. However, this was not focus of the current studies.

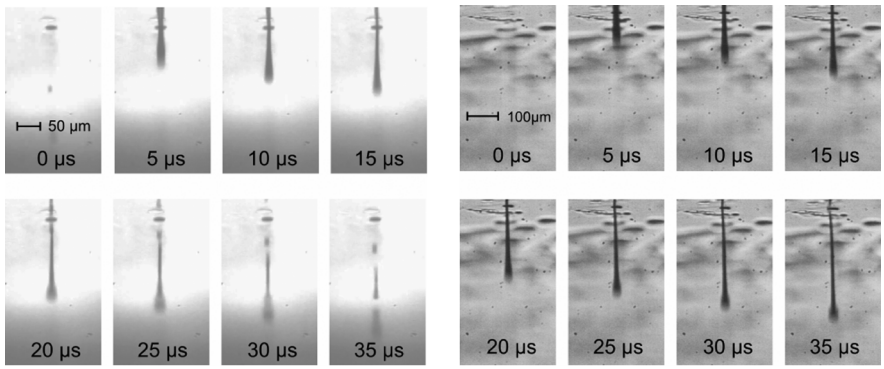

Fig. 8. Ejection cycle of the (a) 1/3-in and (b) 1-in printhead taken by a stroboscopic camera. Every picture is a new ejection with a certain time delay to start signal.

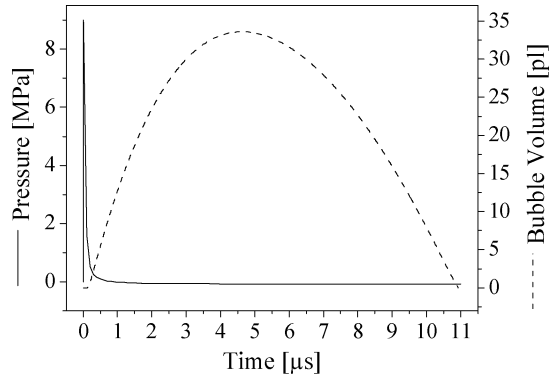

Fig. 9. Pressure pulse used as pressure boundary condition calculated by applying the Clausius–Clapeyron equation and the bubble volume resulting from the simulation.

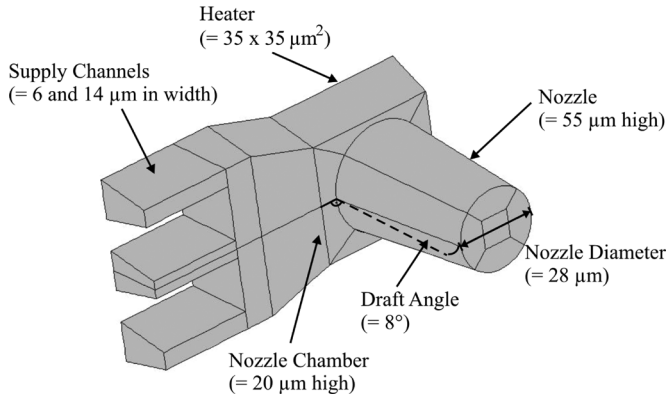

Fig. 10. Schematic drawing of the 3-D model of one nozzle of the 1/3-in bubble jet printhead showing only the fluidic part with corresponding dimensioning.

A. Pressure Boundary Condition

A given current pulse through a microheater of a conventional bubble jet printer can be converted into an equivalent exponential decreasing pressure function following the approach of Asai *et al.* [20]–[24]. The initial pressure of this pressure pulse can be determined using the Clausius–Clapeyron equation [29], [30]

$$P_v[T_v] = P_{\mathrm{atm}} \exp\left[\frac{w \cdot Q_{\mathrm{vap}}}{\mathrm{R}}\left(\frac{1}{T_b} - \frac{1}{T_v}\right)\right] \qquad (1)$$

where P_v and T_v are the approximately uniform pressure and temperature in the vapor bubble, P_{atm} is the atmospheric pressure ($=$ 100 kPa), R is the gas constant ($=$ 8.3148 J mol^{-1} K^{-1}), T_b is the boiling point of the ink, and w and Q_{vap} are molecular weight and heat of vaporization, respectively. Adding a time-dependent heating pulse leads to the following exponentially decreasing pressure function $P_v[t]$, which is displayed in Fig. 9:

$$P_v[t] = P_t(T_t) \exp\left[-\left(\frac{t}{t_0}\right)^{0.5}\right] + P_s(T_{\mathrm{amb}}) \qquad (2)$$

where $P_t(T_t)$ is the initial bubble pressure depending on the maximum heating temperature T_t. In this case, the initial bubble pressure is 9 MPa. P_s is the bubble pressure in the later stage depending on the ambient temperature T_{amb}. The parameter t_0 is a time constant, which has been estimated to be 0.055 μs by calibrating a series of simulations with corresponding experimental results starting from the value of 0.17 μs reported in the literature [20], [23]. This calibration of the model was necessary due to the more complicated three-dimensional geometry compared to the simple assumptions [20], [23], which leads to a different nucleation and bubble collapse.

B. Resulting Bubble Volume

The presented pressure boundary has been applied to the model of different printhead designs under study by substituting the heater area of the real design with an inlet pressure boundary in the simulation using air as incoming medium. The pumped air form the bubble displaces the ink and creates a flow through the nozzle as well as back into the reservoir. The exponential decreasing pressure function results in a parabolic time-dependency of the bubble volume, as displayed in Fig. 9. Maximum bubble volume and time characteristics depend essentially on the printhead geometry and ink properties. These are summarized in the empirical parameter t_0 of Asai's model.

Using the described approach, the simulation results of simple two-dimensional devices presented in the literature [3], [6], [31] could be reproduced easily by using the volume of fluid (VOF) method [32] including surface tension like implemented in ACE+. Afterwards the more complicated 3-D model of an Olivetti I-Jet printhead, as displayed in Fig. 10, and slightly different design variants have been set up to simulate

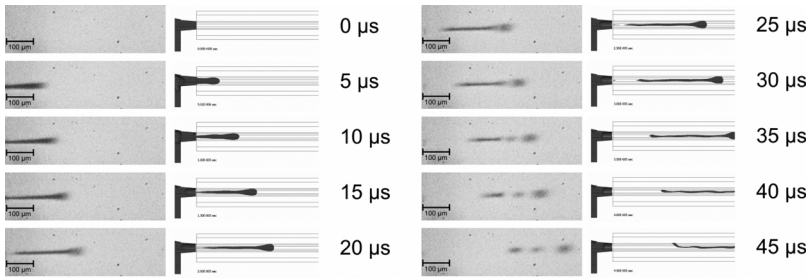

Fig. 11. Comparison of the 3-D simulations of the droplet ejection of a 1/3-in printhead (only the fluidic part is shown) and the corresponding stroboscopic pictures.

a complete dosage cycle including first priming, printing, and refilling. Thus it was possible to simulate the print frequency as well. The simulation of such a complete ejection process took about two days of computing time on a state-of-the-art PC.

C. Simulations Versus Experiments

Comparing the simulations with experimental results like stroboscopic pictures as displayed in Fig. 11, good qualitative agreement has been obtained. The shape of the droplet and the tail look very similar. Also the quantitative agreement between experimental findings and simulations is acceptable: The gravimetrically measured droplet volume of 22 $\pm$ 5 pl is slightly smaller compared to the simulated volume of 30 pl for the nozzle of the 1/3-in printhead. For the 1-in printhead, the simulated droplet volume of 73 pl differs more significantly from the measured volume of about 58 $\pm$ 8 pl. This is caused by the experimental setup used for the 1-in printhead, where the ink feeding channel had a considerably higher fluidic resistance than implemented in the simulation model. Nevertheless, the simulated droplet volumes of 30 and 73 pl, respectively, agree perfectly with the intended droplet volume of the printhead manufacturer.

After this validation of the simulation model, further simulations have been performed to study the printhead performance by varying parameters like geometry dimensions, heating pulse or ink properties. However, this was done only by simulation. No further prototypes were manufactured within this project.

D. Laser Machining and Assembly and Packaging Tolerances

Knowledge of the allowable tolerances is very important for the laser machining and the assembly and packaging of the printhead. Especially the effect of lateral adjustment deviations or differences of chamber height has been studied in detail. The effect of a variation of the nozzle diameter or the draft angle, which are both affected by the laser machining process on the droplet volume and velocity, are displayed in Fig. 12 and 13, respectively. In this case, the intended design is a slight variation of the 1/3-in design depicted in Fig. 10. Due to this, the resulting droplet volume varies a bit compared to previous showed droplet volumes.

The effect of other variations, like an adjustment deviation or an increased height of the adhesive layer on the droplet volume and velocity, is summarized in Fig. 14. As mentioned before, these results are very useful for determination of allowable tolerances for the assembling and packaging.

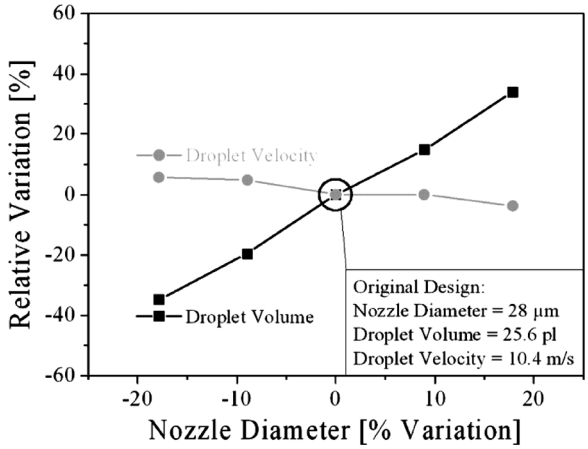

Fig. 12. Simulated effect of varying the nozzle diameter on the droplet volume and velocity.

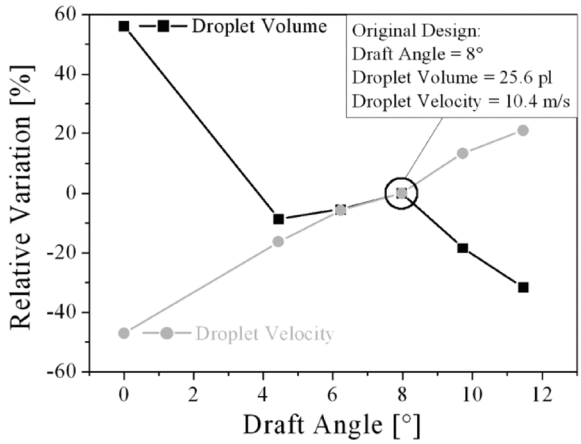

Fig. 13. Simulated effect of varying the draft angle on the droplet volume and velocity.

Summarizing the figures, it can be stated that a small variation of the nozzle chamber height or a minimal deviation of the adjustment leads to a negligible change of the resulting droplet volume and velocity, whereas a deviation of the nozzle diameter or its draft angle induces a more significant change of the ejected droplet volume and velocity. Here a variation of 20% of the nozzle diameter leads to a variation of the droplet volume of 35% and a variation of the droplet velocity of 5%, whereas a variation of 50% of the nozzle diameter leads to a variation of the droplet volume of 30% and a variation of the droplet velocity of 20%.

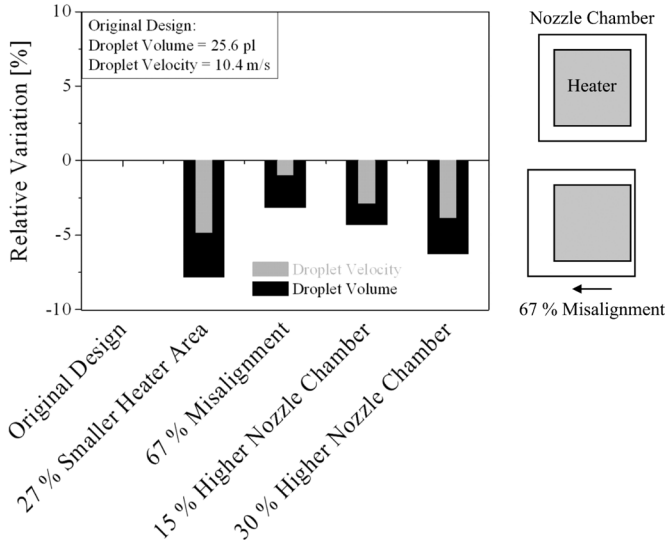

Fig. 14. Comparison of simulated droplet volumes and velocities considering different geometrical tolerances. The 67% misalignment means a misalignment of heater and nozzle chamber of 67% compared to the original distance of them, as displayed in the schematic drawing.

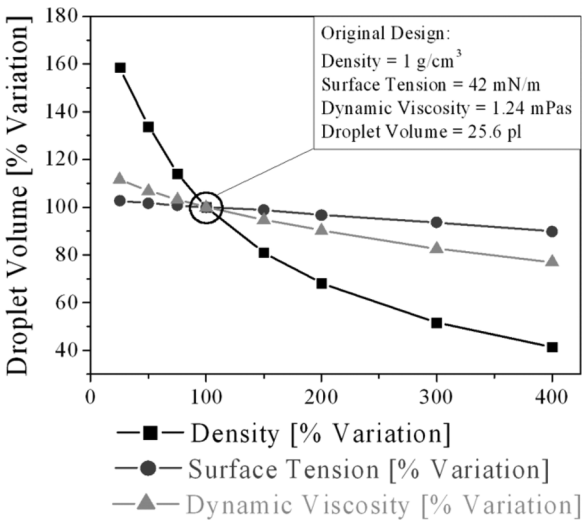

Fig. 15. Simulated droplet volume dependence on the density, the surface tension, and the dynamic viscosity of the ink, respectively.

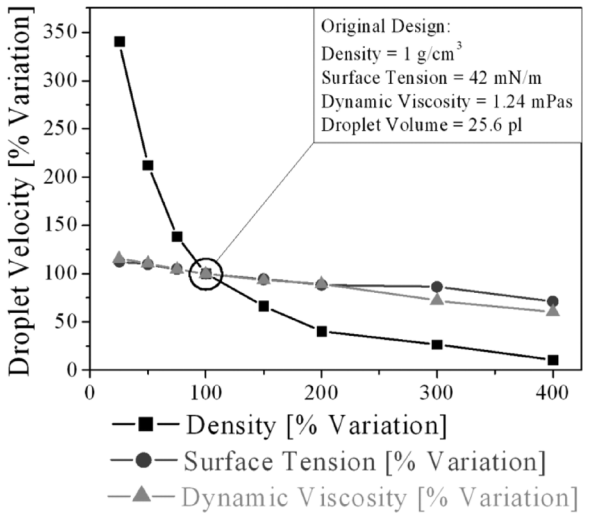

Fig. 16. Simulated droplet velocity dependence on the density, the surface tension, and the dynamic viscosity of the ink, respectively.

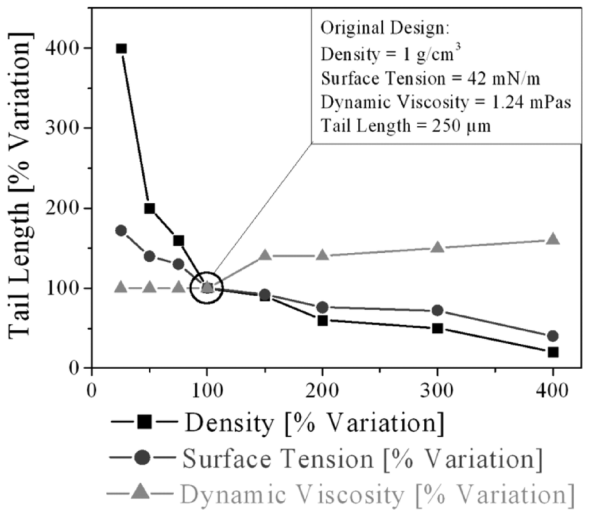

Fig. 17. Simulated tail length of the droplet dependence on the density, the surface tension, and the dynamic viscosity of the ink, respectively.

E. Ink Properties

It is well known that the ink properties play a major role in determining the print volume. Tuning of the ink is the usual method applied to adjust the volume. Varying the ink parameters like density, surface tension, or dynamic viscosity leads to a significant change in the droplet volume, as displayed in Fig. 15. The droplet volume can be halved by increasing the density sixfold. But reducing the droplet volume by varying ink parameters induces also additional changes in the ejection behavior. The droplet velocity, for example, is also very sensitive to fluid properties, especially to the ink density (see Fig. 16). High-density ink leads to very low droplet velocities, which are not desirable. Furthermore, also altering surface tension or viscosity causes a significant change of the velocity.

Another result of the VOF simulations can be deduced by surveying the shape of the ejected droplet and its tail. Tail length and potential satellites are important criteria for the quality of later printouts. The dependence of the tail length on the different ink properties is illustrated in Fig. 17. The bandwidth of the tail length ranges between very long tails (1000 μm) and very short tails. In a very long tail, the tail breaks in some satellites, whereas in very short ones, the tail contracts with the droplet so that no satellites occur. Beyond increasing the print resolution [5]–[7] and realizing a monolithic printhead [3], [4], preventing satellite droplets is an important part of current research and development activities [8], [9].

Admittedly, regarding this results one has to keep in mind that the ink properties cannot be tuned independently. In reality, density, surface tension, and dynamic viscosity are intimately connected. The optimum interaction between printhead geometry and ink parameters has to be found by combining all of the simulation results appropriately.

V. Conclusion

The presented innovative laser machining of a polyimide integrated nozzle plate provides a beneficial manufacturing method for bubble jet printheads in order to meet the requirement of fabricating a low volume, high speed, and wide format inkjet printer. The integration of the channel layer and the nozzle layer in one material and one process step, in contrast to standard manufacturing methods, offers better accuracy and saves one alignment step.

Furthermore, an assembling method using an adhesive layer of only 3 μm thickness with an alignment accuracy of 5 μm was presented. The method was applied to fabricate a printhead with integrated nozzle plate of 1-in size for the first time. The samples produced with 1/3- and 1-in nozzle plates, respectively, exhibited a good impermeability, robust capillary filling, long—term stability, and satisfactory droplet quality.

The presented three-dimensional simulation model of the thermal ink jet printhead provides a valuable approach to improve the efficiency of thermal bubble jet printheads regarding droplet volume, droplet velocity, droplet quality, and print frequency, also including the consideration of 3-D sensitive aspects. The correctness of the used pressure boundary condition and the simulation model in the three-dimensional case was verified by comparing simulations with gravimetrical and stroboscopic results. For the optimization or the designing of a new printhead, a variety of specific models may be investigated by adjusting all relevant parameters like geometry effects and ink properties.

Acknowledgment

The authors would like to thank T. Goettsche (HSG-IMIT), R.-P. Peters (Boehringer Ingelheim microParts), A. Bellone, and A. Scardovi (both Olivetti I-Jet) for support of the work reported in this paper.

References

[1] S. Zoltan, "Printing head for ink jet printer," U.S. Patent 4 641 155, 1987.

[2] J. L. Vaught, F. L. Cloutier, D. K. Donald, J. D. Meyer, C. A. Tacklind, and H. H. Taub, "Thermal ink jet printer," U.S. Patent 4 490 728, 1984.

[3] S. S. Baek, H. T. Lim, H. Song, Y. S. Kim, K. D. Bae, C. H. Cho, C. S. Lee, J. W. Shin, S. J. Shin, K. Kuk, and Y. S. Oh, "T-Jet: A novel thermal inkjet printhead with monolithically fabricated nozzle plate on SOI wafer," in *Proc. IEEE Transducers*, 2003, pp. 472–475.

[4] Y.-J. Chuang, F. G. Tseng, and W.-K. Lin, "A thermal droplet generator with monolithic photopolymer nozzle plate," in *Proc. IEEE Transducers*, 2003, pp. 476–479.

[5] M. Murata, M. Kataoka, R. Nayve, A. Fukugawa, Y. Ueda, T. Mihara, M. Fujii, and T. Iwamori, "High resolution long array thermal ink jet printhead with on-chip LSI heater plate and micromachined Si channel plate," *IEICE Trans. Electron.*, vol. E84C, no. 12, pp. 1792–1800, 2001.

[6] R. Nayve, M. Fujii, A. Fukugawa, and M. Murata, "High resolution long array thermal ink jet printhead fabricated by anisotropic wet etching and deep Si RIE," in *Proc. IEEE Int. Conf. Micro Electro Mech. Syst. (MEMS)*, 2003, pp. 456–461.

[7] R. Nayve, M. Fujii, A. Fukugawa, T. Takeuchi, M. Murata, Y. Yamada, and M. Koyanagi, "High-resolution long-array thermal ink jet printhead fabricated by anisotropic wet etching and deep Si RIE," *J. Microelectromech. Syst.*, vol. 13, no. 5, pp. 814–821, 2004.

[8] F. G. Tseng, C. J. Kim, and C. M. Ho, "A high-resolution high-frequency monolithic top-shooting microinjector free of satellite drops—Part I: Concept, design, and model," *J. Microelectromech. Syst.*, vol. 11, no. 5, pp. 427–436, 2002.

[9] ——, "A high-resolution high-frequency monolithic top-shooting microinjector free of satellite drops—Part II: Fabrication, implementation, and characterization," *J. Microelectromech. Syst.*, vol. 11, no. 5, pp. 437–447, 2002.

[10] R. Conta and A. Scardovi, "Printhead with multiple ink feeding channels," Int. Patent WO 0 147 715 A1, 2001.

[11] T. Lizotte, O. Ohar, and S. C. Waters, "Excimer lasers drill inkjet nozzles," *Laser Focus World*, vol. 38, no. 5, pp. 165–168, 2002.

[12] R. R. Allen, J. D. Meyer, and W. R. Knight, "Thermodynamics and hydrodynamics of thermal ink jets," *Hewlett-Packard J.*, vol. 36, no. 5, pp. 21–27, 1985.

[13] J. D. Beasley, "Model for fluid ejection and refill in an impulse drive jet," *Photograph. Sci. Eng.*, vol. 21, no. 2, pp. 78–82, 1977.

[14] N. V. Deshpande, "Significance of inertance and resistance in fluidics of thermal ink-jet transducers," *J. Imag. Sci. Technol.*, vol. 40, no. 5, pp. 396–400, 1996.

[15] J. E. Fromm, "Numerical-calculation of the fluid-dynamics of drop-on-demand jets," *IBM J. Res. Develop.*, vol. 28, no. 3, pp. 322–333, 1984.

[16] C. Rembe, S. aus der Wiesche, and E. P. Hofer, "Thermal ink jet dynamics: Modeling, simulation, and testing," *Microelectron. Reliab.*, vol. 40, no. 3, pp. 525–532, 2000.

[17] S. aus der Wiesche, C. Rembe, and E. P. Hofer, "Boiling of superheated liquids near the spinodal—II: Application," *Heat Mass Transfer*, vol. 35, no. 2, pp. 143–147, 1999.

[18] S. aus der Wiesche, C. Rembe, and E. P. Hofer, "Boiling of superheated liquids near the spinodal—I: General theory," *Heat Mass Transfer*, vol. 35, no. 1, pp. 25–31, 1999.

[19] Z. Zhao, S. Glod, and D. Poulikakos, "Pressure and power generation during explosive vaporization on a thin-film microheater," *Int. J. Heat Mass Transfer*, vol. 43, no. 2, pp. 281–296, 2000.

[20] A. Asai, T. Hara, and I. Endo, "One-dimensional model of bubble-growth and liquid flow in bubble jet printers," *Jpn. J. Appl. Phys. Part 1—Regular Papers Short Notes Rev. Papers*, vol. 26, no. 10, pp. 1794–1801, 1987.

[21] A. Asai, S. Hirasawa, and I. Endo, "Bubble generation mechanism in the bubble jet recording process," *J. Imag. Technol.*, vol. 14, no. 5, pp. 120–124, 1988.

[22] A. Asai, "Application of the nucleation theory to the design of bubble jet printers," *Jpn. J. Appl. Phys. Part 1—Regular Papers Short Notes Rev. Papers*, vol. 28, no. 5, pp. 909–915, 1989.

[23] ——, "Bubble dynamics in boiling under high heat-flux pulse heating," *J. Heat Transfer Trans. ASME*, vol. 113, no. 4, pp. 973–979, 1991.

[24] ——, "3-dimensional calculation of bubble-growth and drop ejection in a bubble jet printer," *J. Fluids Eng. Trans. ASME*, vol. 114, no. 4, pp. 638–641, 1992.

[25] CFD-ACE+ (ESI-Group) [Online]. Available: http://esi-group.com [Online]. Available: http://www.cfdrc.com, 2004

[26] T. Lindemann, D. Sassano, A. Bellone, R. Zengerle, and P. Koltay, "Three-dimensional CFD-simulation of a thermal bubble jet printhead," in *Tech. Proc. 2004 NSTI Nanotechnol. Conf. Trade Show*, 2004, pp. 227–230.

[27] T. Lindemann, H. Ashauer, T. Goettsche, H. Sandmaier, Y. Yu, R.-P. Peters, D. Sassano, A. Bellone, A. Scardovi, R. Zengerle, and P. Koltay, "Thermal bubble jet printhead with integrated nozzle plate," in *Proc. Int. Conf. Digital Printing Technol. 2004 (NIP20)*, 2004, pp. 834–839.

[28] T. Lindemann, H. Ashauer, T. Goettsche, H. Sandmaier, Y. Yu, R.-P. Peters, D. Sassano, A. Bellone, R. Zengerle, and P. Koltay, "Bubble jet printhead with integrated polyimide nozzle plate," in *Proc. 18th IEEE Int. Conf. Micro Electro Mech. Syst. (MEMS 2005)*, 2005, pp. 560–563.

[29] R. L. Lide, *Handbook of Chemistry and Physics*, 82nd ed. Boca Raton, FL: CRC Press, 2001.

[30] H. Stöcker, *Taschenbuch der Physik*, 3 ed. Thun und Frankfurt am Main, Germany: Verlag Harri Deutsch, 1998.

[31] P. H. Chen, W. C. Chen, and S. H. Chang, "Bubble growth and ink ejection process of a thermal ink jet printhead," *Int. J. Mech. Sci.*, vol. 39, no. 6, p. 683, 1997.

[32] C. W. Hirt and B. D. Nichols, "Volume of fluid (Vof) method for the dynamics of free boundaries," *J. Comp. Phys.*, vol. 39, no. 1, pp. 201–225, 1981.

Timo Lindemann received the degree in engineering in microsystem technologies and the Ph.D. degree from the Department of Microsystems Engineering (IMTEK), University of Freiburg, Germany, in 2002 and 2006, respectively.

From August 2002 until February 2006, he was with the Microfluidics Simulation Group, IMTEK, Laboratory for MEMS Applications. His dissertation is on "Droplet Generation: From the Nanoliter to the Femtoliter Range" in which he pioneers the use of computational fluid dynamics (CFD) simulation tools to study the droplet release processes in various dispensing technologies developed at the laboratory. Among those are inkjet dispensers, the TopSpot and dispensing well plate technology, the PipeJet dispenser, and aerosol generators. Since February 2006, he has been with the Department of Corporate Sector Research and Advance Engineering, Microsystem Technologies, Robert Bosch GmbH, Stuttgart, Germany.

Heidi Ashauer received the degree in engineering from the Technical University Chemnitz, Germany, in 1975.

In 1976, she joined Technikum Mikroelektronik, Technical University Chemnitz, where she was mainly engaged in research and development of microelectronic and microsystem technology. She joined HSG-IMIT, Villingen-Schwenningen, Germany, in 1991, where she is currently a Research and Development Engineer for assembly and packaging in the field of MEMS. Her research interests are new packaging techniques for MEMS.

Ying Yu (M'96) was born in Tianjin, China, in 1955. He received the electrical engineering degree from the Electrical Engineering Department, University Tianjin, China, in 1982; the engineer diploma from the Electrical Engineering Department, University Dortmund, Germany, in 1986, and the Ph.D degree in mechanical engineering from the Technical University Berlin, Germany, in 1992.

He was a Research Assistant from 1987 to 1990 in the Institute of Fine-Mechanical Technology and Biomedical Technology, Technical University Berlin. Within this time he published "Electrical signal processing for force compensated sensors," Symposium on Planar-Technology for Printer and Scanner, in 1988. Since 1990, he has been a Project Manager in the field of MEMS with Boehringer Ingelheim microParts GmbH (former STEAG microParts GmbH). His research and development activities include LIGA technology, inkjet technology, microelectronics, laser micromachining, rapid prototyping of microstructures and design of microstructures for microfluidics, especially for biomedical applications.

Duccio Spartaco Sassano was born in Ivrea, Italy, on July 18, 1963. He studied electronics at Turin Politechnic, Italy.

With Olivetti (now Italian Telecom Group) he started in inkjet R&D and became printhead microhydraulic Project Manager. He has also been involved with Olivetti inkjet products integration (AIO, fax, new inkjet applications). He frequently attends Society for Imaging Science and Technology and Information Management Institute conferences and has taken part in several European research projects.

Roland Zengerle is Head of the Laboratory for MEMS Applications at the Department of Microsystems Engineering (IMTEK), University of Freiburg, Germany. He also is a Director with the Institute for Micro- and Information Technology, Hahn-Schickard-Gesellschaft (HSG-IMIT), a nonprofit organization supporting industries in development of new products based on MEMS technologies.

His and his team's research is focused on microfluidics and covers topics such as miniaturized and autonomous dosage systems, implantable drug delivery systems, nanoliter and picoliter dispensing, lab-on-a-chip systems, thermal sensors, miniaturized fuel cells, and micro- and nanofluidics simulation. He has coauthored more than 200 technical publications and 25 patents. He is the European Editor of the *Springer Journal of Microfluidics and Nanofluidics.* He is a member of the Technical Program Committee of several international conferences.

Dr. Zengerle is a member of the International Steering Committee of the IEEE-MEMS conference.

Peter Koltay studied physics at the University of Freiburg, Germany, and the University of Budapest, Hungary. He received the Ph.D. degree from the University of Freiburg in 1999.

He joined the Department of Microsystems Engineering (IMTEK), University of Freiburg, where he is heading the Picoliter and Nanoliter Dispensers Group and the group on Fluidic Simulation. His research interests are especially related to the development of microfluidic liquid-handing devices for various life-science applications as, for example, microdispensers, modeling of free surface flows, and simulation of microfluidic devices by system simulation and computational fluid dynamic simulation. Since 2005, he has been Managing Director of BioFluidix GmbH dealing with the commercialization of micro dispensing technologies developed by IMTEK and HSG-IMIT.